Bifurcation lesions
Fundamental aspects

European Bifurcation Club

EBC

Andrejs Erglis MD, PhD
Latvian Centre of Cardiology
Riga, LATVIA

Geometry of bifurcation

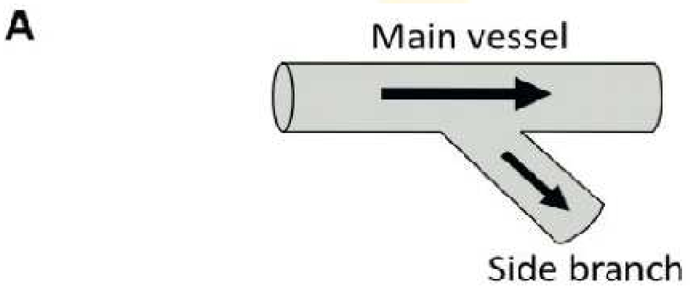

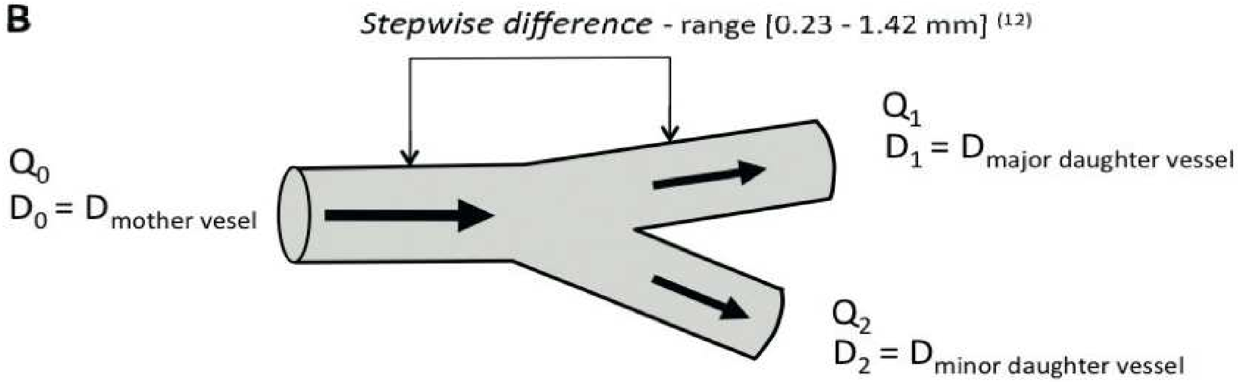

Law of flow (mass) conservation	$Q_0 = Q_1 + Q_2$
Murray's law (7)	$D_0^3 = D_1^3 + D_2^3$
HK 7/3 model (11)	$D_0^{7/3} = D_1^{7/3} + D_2^{7/3}$
Linear law (12) (epicardial coronary artery)	$D_0 = 0.678 * (D_1 + D_2)$

A) A conventional schema, in which the "main vessel" diameter is conserved before and after the origin of "side branch", which is false.

B) True representation of a bifurcation, with a mother vessel dividing into two daughter vessels. Strict relations are obtained between the flow rates and diameters of the three vessels, in agreement with the law of conservation of mass (or flow). The diameter of the mother vessel is systematically greater than that of the larger daughter vessel.

The greater the difference in diameter between the two daughter vessels, the greater the systematic stepwise difference between the diameters of the mother and major daughter vessels.

Finet G et al. *EuroIntervention.* 2010;6 Suppl J: J10-J15

Bifurcation impact on fluid dynamics

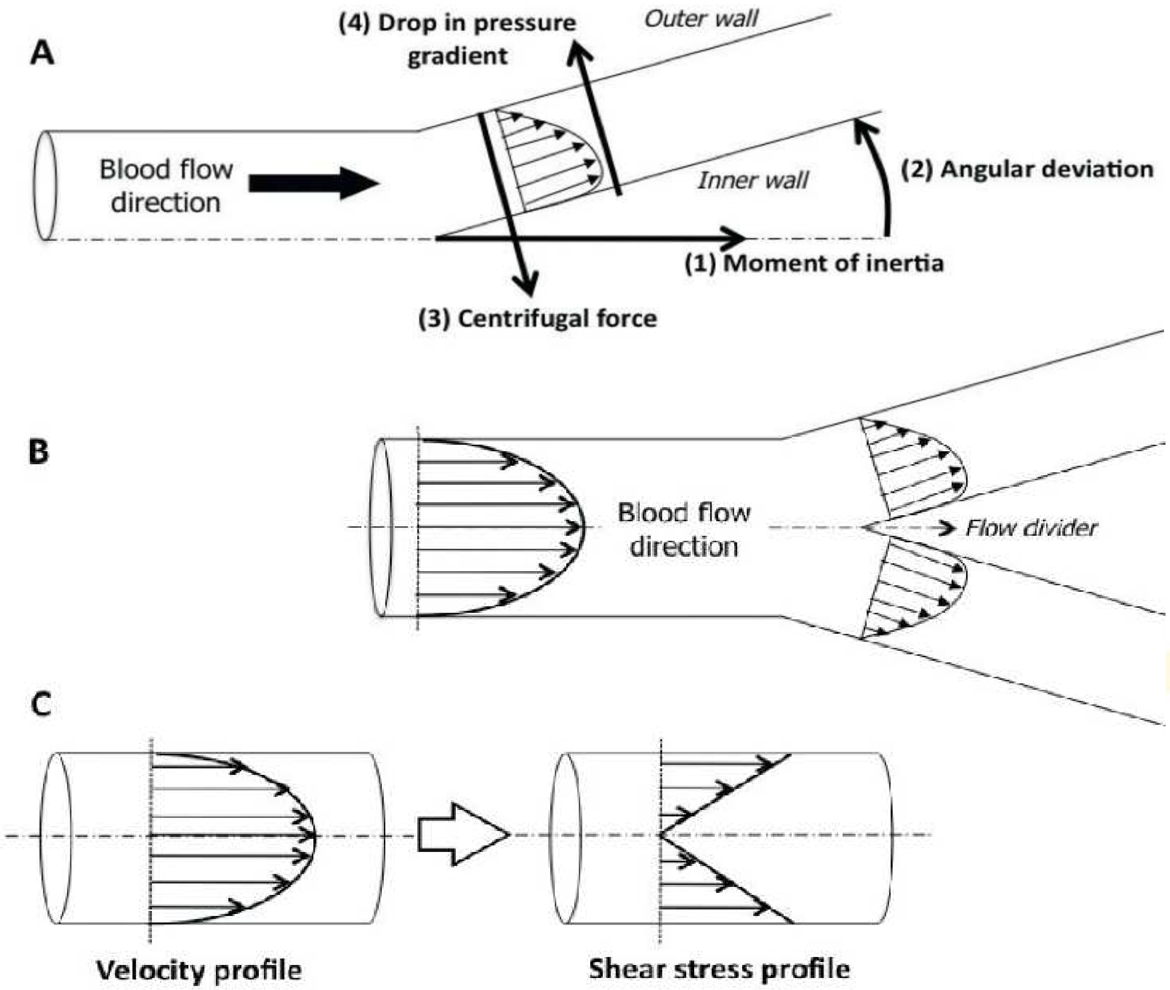

A) Laminar flow in an artery induces a force of inertia (1) in the direction of flow; a sudden change in direction characterised by an angular deviation (2) induces a centrifugal force (3) which creates a pressure gradient at the exit from the change in direction.

B) Description of fluid dynamics changes from symmetric laminar flow before the bifurcation to asymmetric flow gradients after division of the flow.

C) The flow velocity profile is associated with a shear stress profile, corresponding to the derivative of the velocities from their radial position.

Finet G et al. *EuroIntervention.* 2010;6 Suppl J: J10-J15

Wall shear stress in bifurcations

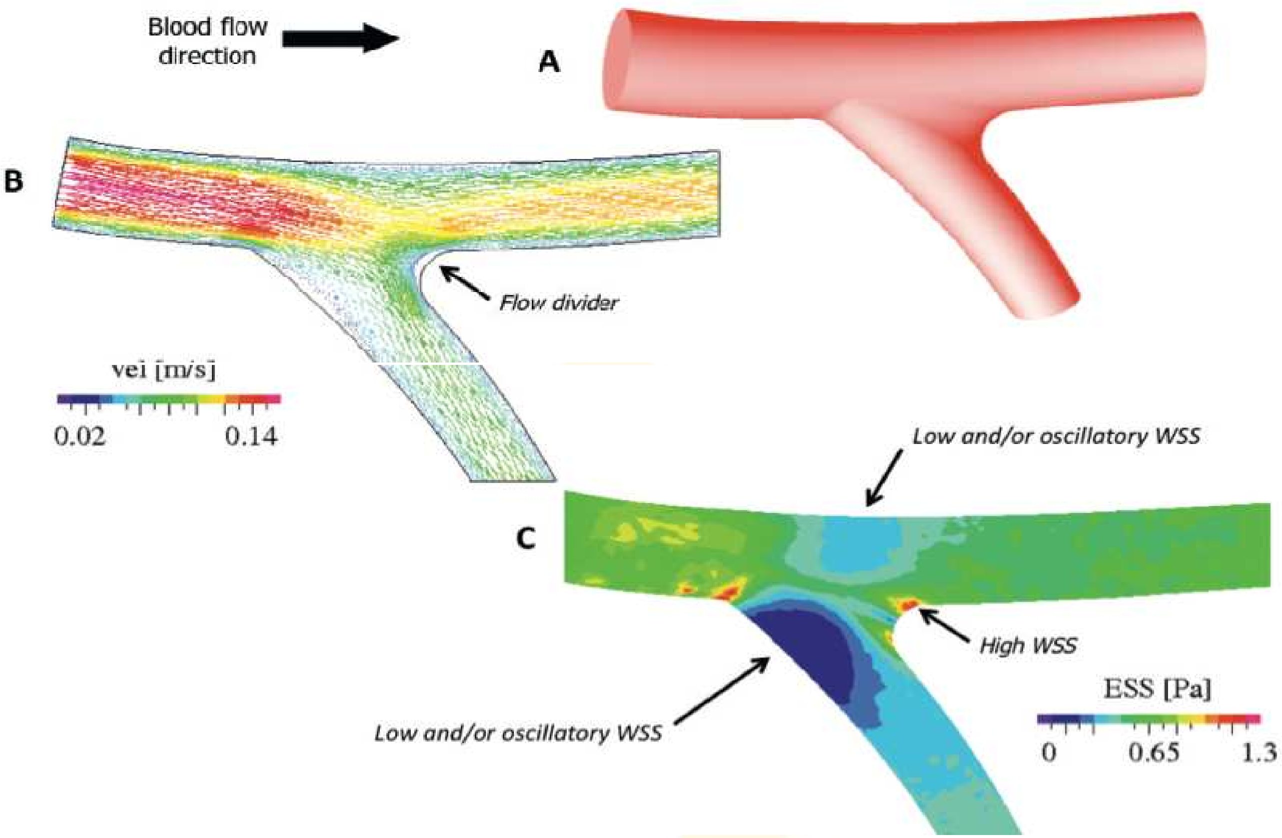

A) The coronary bifurcation model respects a fractal geometry.
B) Map of velocity profile, showing the preferential route towards the flow divider induced by the force of inertia.
C) Map of wall shear stress (WSS) showing two contrasting regions at the flow divider where WSS is low, regions where flow is very slow and/or oscillatory.

Finet G et al. *EuroIntervention.* 2010;6 Suppl J: J10-J15

Role of low shear stress in atherosclerosis

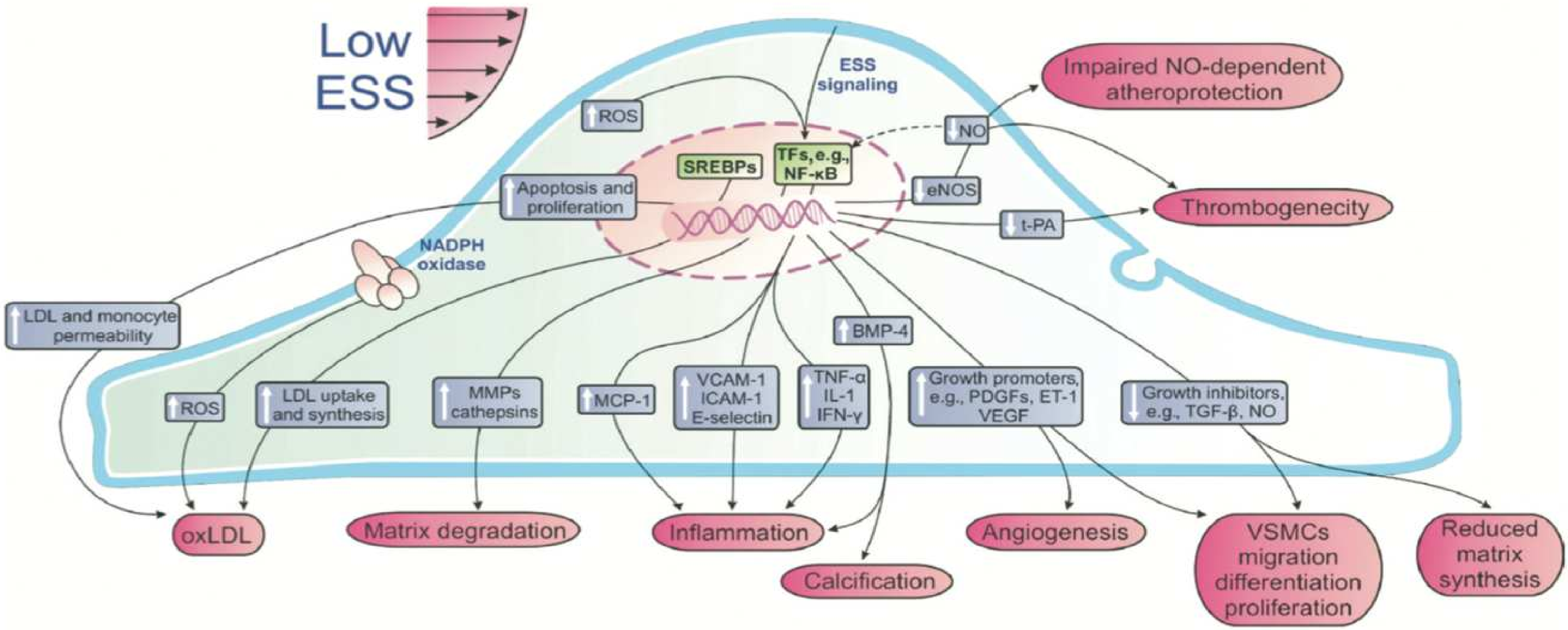

Chatzizisis YS et al. *J Am Coll Cardiol* 2007;49:2379–93
Giannoglou GD et al. *EuroIntervention.* 2010;6 Suppl J: J16-J23

Impact of flow on atheroma in bifurcation

Flow behavior with low shear regions in the lateral walls and high shear regions at the carina.

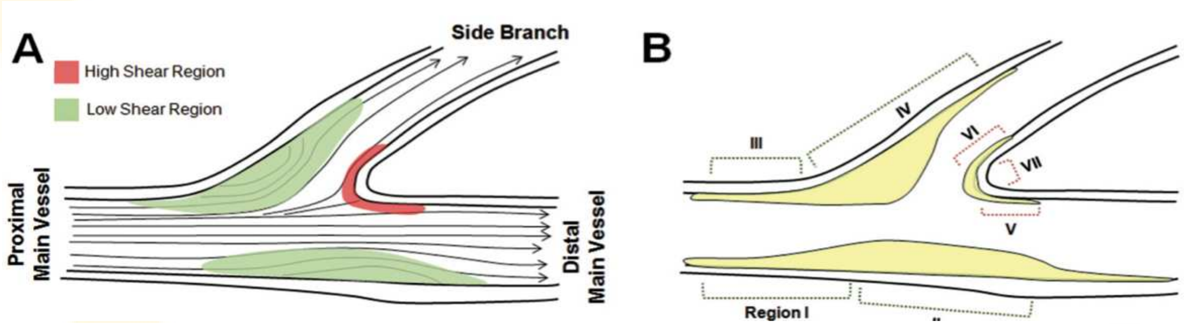

Regions: I - Proximal MV, II - Distal MV on the lateral wall, III - Proximal MV on the SB, IV - Distal SB on the lateral wall, V - Distal MV on the flow divider side, VI - Distal SB on the flow divider side, VII – Carina.

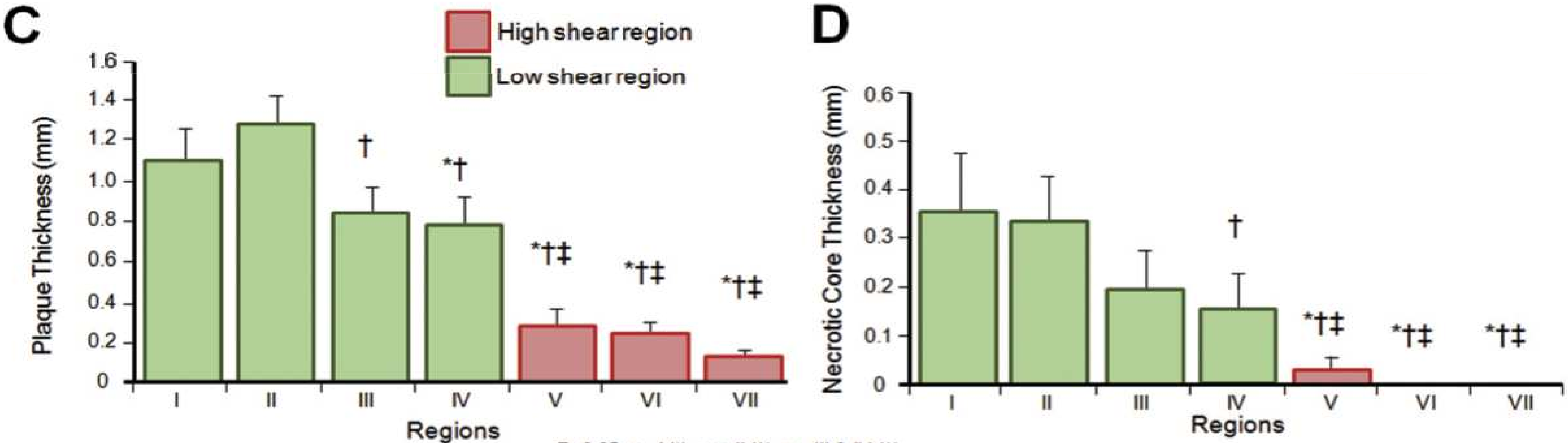

P<0.05, vs. I (*) , vs. II (†), vs. III & IV (‡)

C: Plaque thickness was greater in regions of low shear as compared to high shear.
D: Necrotic core thickness was significantly greater in low shear regions as compared to high shear with absent of necrotic core at the carinal region (VII)

Nakazawa G, Virmani R et al. J Am Coll Cardiol 2010;55:1679–87
Yazdani SK, Virmani R et al. *EuroIntervention.* 2010;6 Suppl J: J24-J30

Impact of flow on arterial healing after stenting

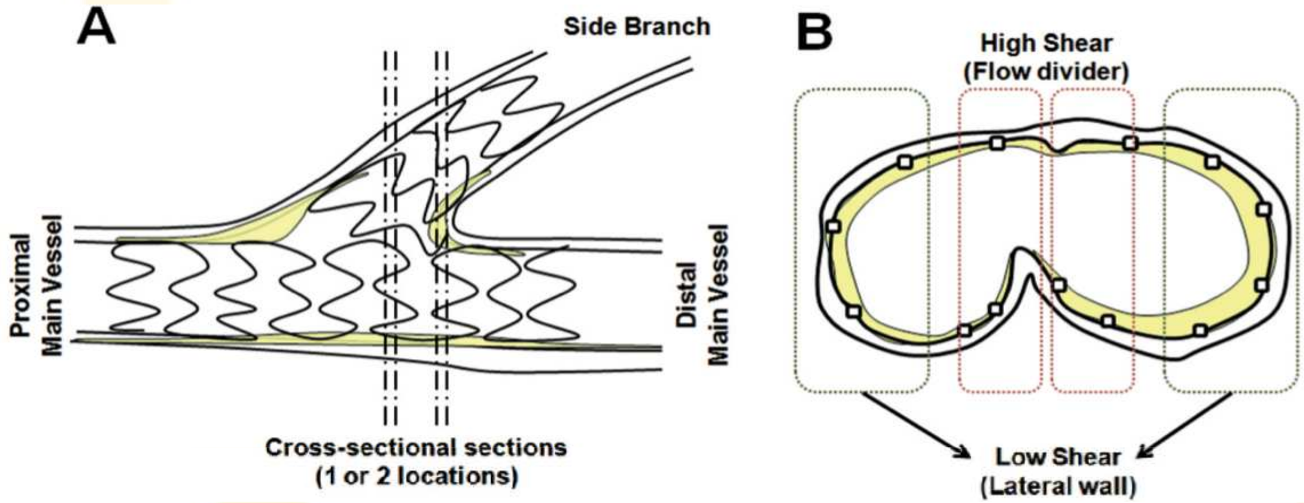

Table 2. Morphometric comparison between high shear vs. low shear regions in DES and BMS.

	DES (12 lesion, 17 stents)		p value	BMS (14 lesion, 18 stents)		p value	P value for DES vs. BMS	
	High shear (flow divider)	Low shear (lateral walls)		High shear (flow divider)	Low shear (lateral walls)		High shear	Low shear
Neointimal thickness (mm)	0.07 [0.03, 0.15]	0.17 [0.09, 0.23]	0.001	0.26 [0.16, 0.73]	0.44 [0.17, 0.67]	0.25	0.0002	0.004
Fibrin deposition (%Struts)	60 [21, 67]	17 [0, 55]	0.01	8 [0, 33]	3 [0, 21]	0.21	0.008	0.19
Uncovered struts (%Struts)	40 [16, 76]	0 [0, 15]	0.001	0 [0, 21]	0 [0, 0]	0.10	0.004	0.38

DES: drug-eluting stent; BMS: bare metal stent; Values are expressed as median and interquartile range

Nakazawa G, Virmani R et al. J Am Coll Cardiol 2010;55:1679–87
Yazdani SK, Virmani R et al. *EuroIntervention.* 2010;6 Suppl J: J24-J30

Intravascular imaging for bifurcations

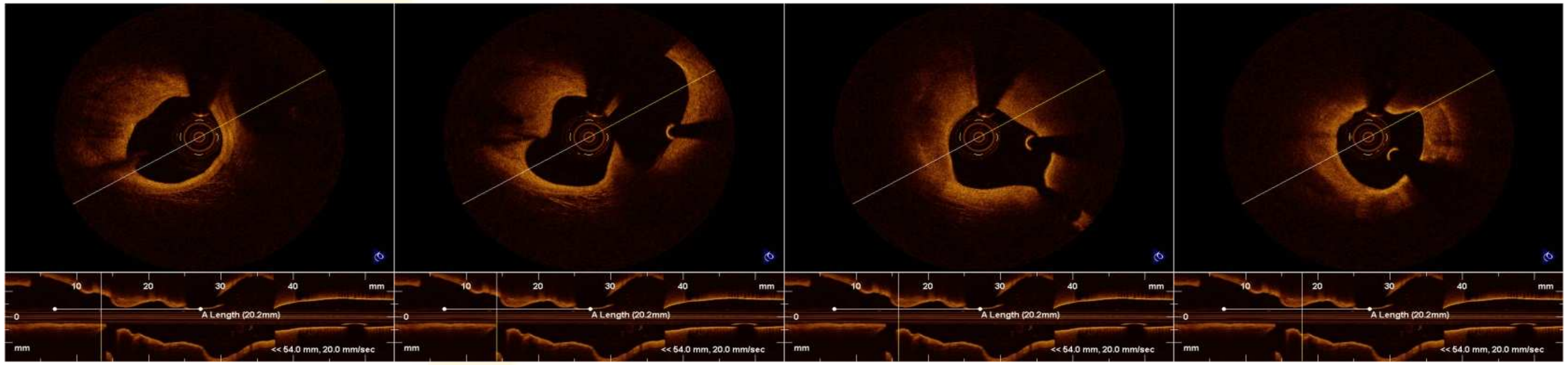

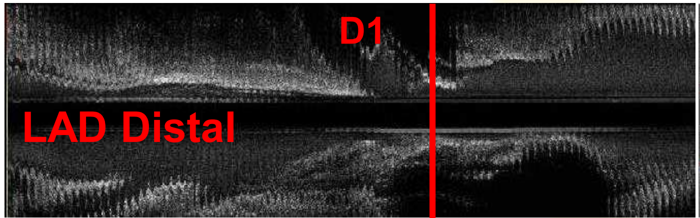

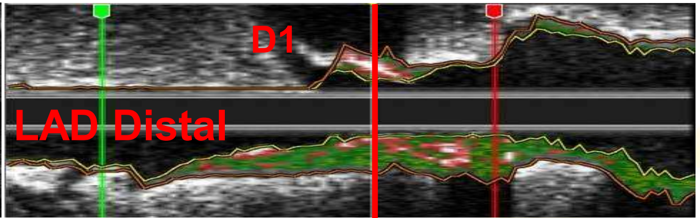

Measurements On Current Frame

	Area (mm²)	Mean	Min	Max	Min/Max
Lumen	3.60	2.17	2.01	2.42	0.83
Vessel	20.32	5.11	4.88	5.42	0.90
Stent					
Plaque	16.72 (82.3% of Vessel)				
NIH					
Malapp					

Diameter (mm)

Volume [mm³]

Lumen Vol
Stent Vol
Plaque Vol
Intimal Vol
Native Plaque
Malapposition
Vessel Vol

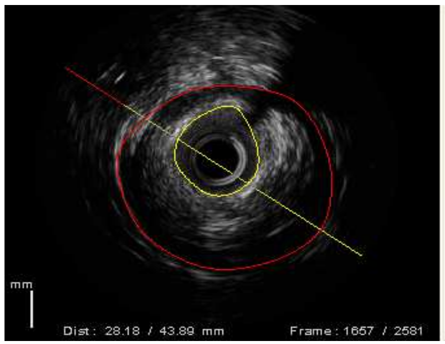

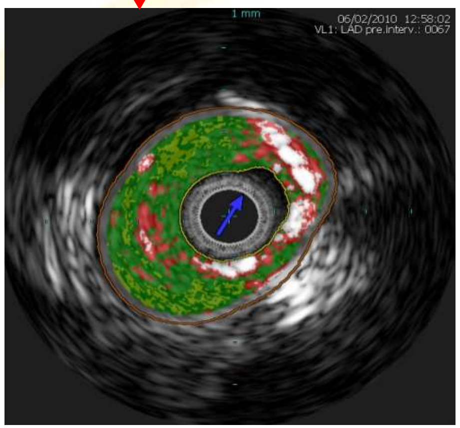

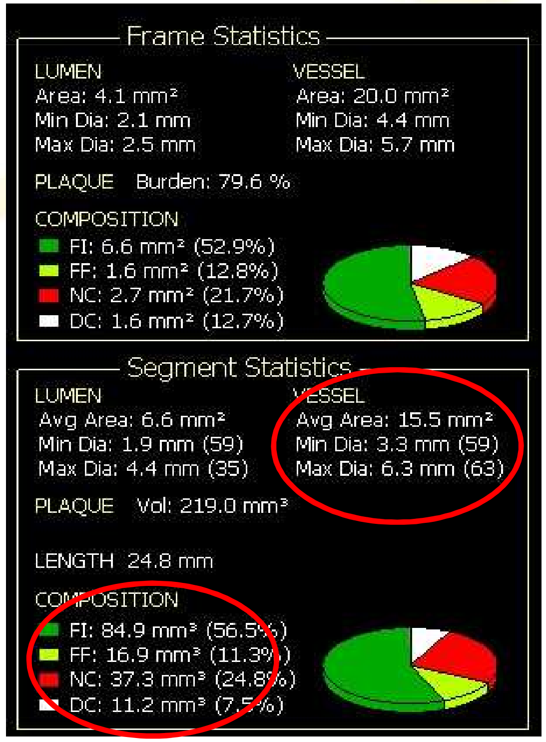

Correlation Between FFR and % Stenosis (QCA) in Jailed Side Branches

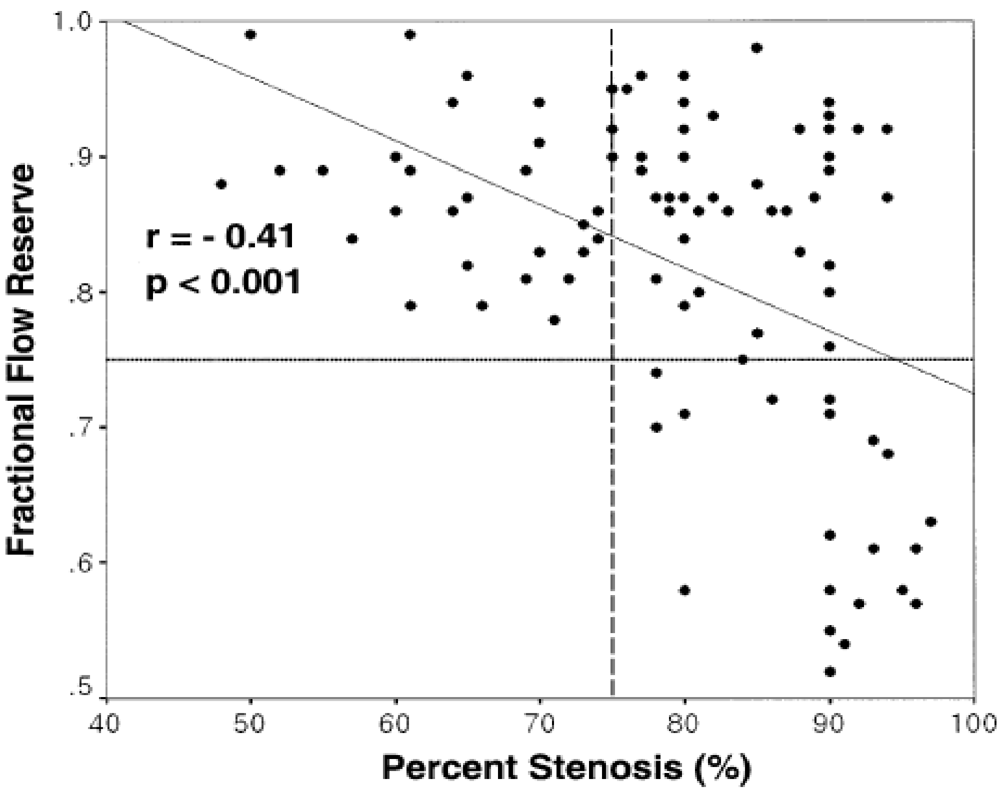

There was a negative correlation between the percent stenosis and FFR (r=0.41, p<0.001).

No lesion with <75% stenosis had FFR<0.75.

Among 73 lesions with ≥75% stenosis, only 20 lesions were functionally significant.

FFR measurements demonstrate that most of stenotic SB do not have functional significance

Koo BK et al *J Am Coll Cardiol* 2005;46:633–7)

Non-invasive CT derived FFR

Anatomic model derived from CCTA

3-D anatomic model extracted from CCTA

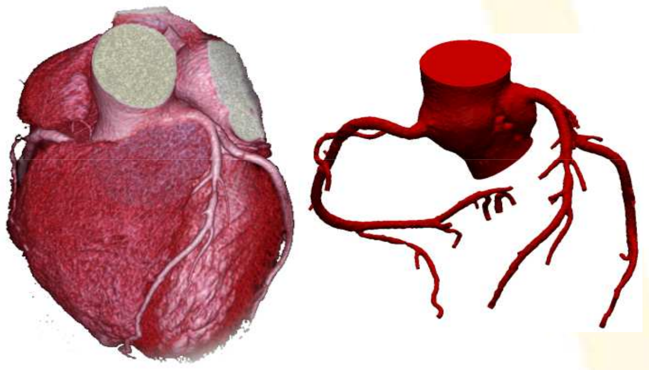

Physiologic modeling considerations:

- Aortic pressure
- Myocardial demand
- Coronary morphometry
- Known vasodilatory effect of adenosine

Blood Flow Solution

Blood flow equations are solved on a supercomputer to provide coronary artery **pressure** and **flow**.

$$\rho \bar{v}_{,t} + \rho \bar{v} \cdot \nabla \bar{v} = -\nabla p + \nabla \cdot \underset{\sim}{\tau}$$
$$\nabla \cdot \bar{v} = 0$$

Hyperemic flow conditions are simulated in computational model

Computed FFR_{CT}

3-D FFR map computed with FFR values at all points in coronary artery tree

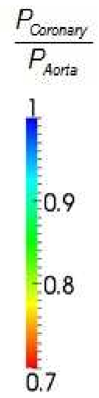

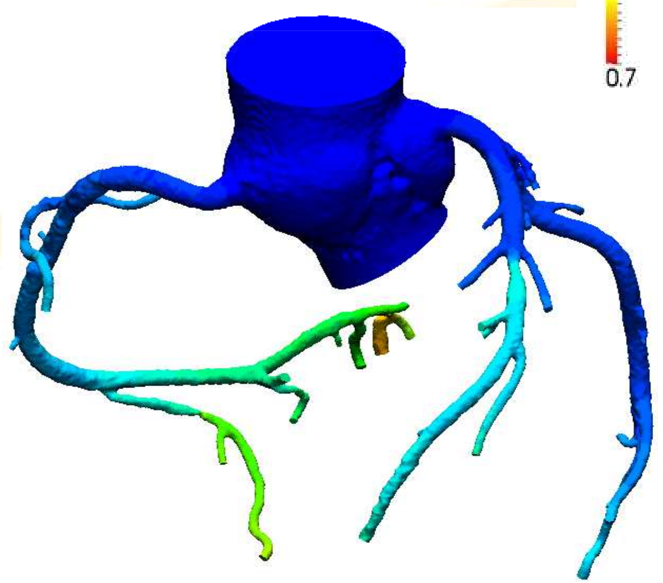

Conclusions

- Bifurcations is the art of geometry, fluid dynamics and rheology.
- On the other hand, atherosclerosis, plaque vulnerability and thrombosis are closely associated with the geometric and fluid dynamics factors at the bifurcation.
- Advances in the current imaging modalities will enable the development of more accurate models for the study of geometry and flow conditions in coronary bifurcations.

HeartFlow™